Enforced expression of *PPP1R13L* increases tumorigenesis and invasion through p53-dependent and p53-independent mechanisms

Magdalena J. Laska[1,2], Scott Lowe[1] , , Lars Zender[1], Stephen Hearn[1], Ulla Vogel[3, 4] , Uffe Birk Jensen[2], Anka Bric[1] , Bjørn A. Nexø[2].

1 Cold Spring Harbor Laboratory, 1 Bungtown Road, Cold Spring Harbor, NY , USA
2 Institute of Human Genetics, University of Aarhus, DK-8000 Aarhus C, Denmark
3 National Institute for the Work Environment, DK-2100 Copenhagen O, Denmark
4 Present address: National Food Institute, DK-2860 Søborg, Denmark

Keywords: *PPP1R13L* gene, malignant transformation, tumorigenesis, tumor celll migration, Tumor suppressor p53.

Running title: ***PPP1R13L* in tumorigenesis and metastasis**

Abstract

PPP1R13L was initially identified as a protein that binds to the NF-κB subunit p65/RelA and inhibits its transcriptional activity. It also binds p53 and inhibits its action. One set of experimental findings based on over-expression of PPP1R13L indicates that PPP1R13L blocks apoptosis. Another set of experiments, based on endogenous production of PPP1R13L, suggests that the protein may sometimes be pro-apoptotic. We have used primary mouse embryonic fibroblasts (MEF's), dually transformed by H-ras and Adenovirus E1A and differing in their p53 status, to explore the effects of PPP1R13L over-expression, thus examining the ability of PPP1R13L to act as an oncoprotein. We found that over-expression of PPP1R13L strongly accelerated tumor formation by ras/E1A and also resulted in an increased metastatic potential of the tumors. PPP1R13L over-expressing cells were depleted for both p53 and active p65/RelA and we found that both, p53 dependent and independent apoptosis pathways, were regulated by PPP1R13L. Finally, studies with the proteasome inhibitor MG132 revealed that over-expression of PPP1R13L causes faster p53 degradation, a likely explanation for the depletion of p53. Taken together, our results show that increased levels of PPP1R13L can increase tumorigenesis and furthermore pinpoint PPP1R13L as a gene that influences metastasis.

Introduction

The recently discovered Apoptosis Stimulating Proteins of p53 (ASPP) family consists of three members, **ASPP1, ASPP2**, and the most evolutionary conserved **PPP1R13L (iASPP),** also known as RAI (Trigiante and Lu, 2006; Slee and Lu, 2003). The three factors are encoded by the genes PPP1R13B, TP53BP2 and PPP1R13L, respectively. The family of proteins is characterized by a highly conserved carboxyl terminus-ankyrin repeats, SH3 (Src homology 3) domain and a proline-rich region. The proteins are thought to bind though these structures to several other proteins, including the tumor suppressor protein p53, BCL2, RelA/p65, protein phoshatase 1, YES- associated protein (Trigiante and XinLu, 2006).

To date, the most well-known function of the ASPP1 and ASPP2 proteins is their ability to induce apoptosis via p53 and its family members, p63 and p73 (Bergamaschi at el., 2003). ASPP1 and ASPP2 enhance the ability of p53 to induce apoptosis by binding to p53 and causing it to specifically upregulate the expression of pro-apoptotic genes rather than genes involved in cell cycle arrest (Bergamashi at el., 2003).

The third family member, PPP1R13L was initially identified and characterized as a novel RelA-associated inhibitor that binds to the NF-κB subunit p65/RelA and inhibits its transcriptional activity (Yang et al., 1999).

Later it has become clear that PPP1R13L also binds to p53. Indeed, in the nematode C. elegans the primary role of Ce-iASPP is to inhibit the pro-apoptotic activity of Ce-p53, which is normally stimulated in response to genotoxic stress. It is unknown if this finding can be generalized to other higher eukaryotes, as C. elegans lack NF-κB, so that the second major arm of pathway is missing. Indeed, two schools of thought exist regarding the primary role of PPP1R13L in mammals. The larger set of experimental findings, which are mainly based on constitutive over-expression of PPP1R13L in transformed cells transfected with the relevant cDNA, indicate that the protein blocks apoptosis, presumably by binding and blocking p53 (Bergamaschi, D., et al. 2003). A smaller set of experiments, based on endogonous production of PPP1R13L, suggests that PPP1R13L may actually be pro-apoptotic (Laska at al., 2007). Both set of findings could very well be true and reflect different roles at different concentration levels and putative activation levels in different cells. To resolve these issues it would be helpful to know the relative affinity of PPP1R13L for p53 and p65/RelA.

Overexpression of PPP1R13L was detected in eight human breast carcinomas expressing wild-type p53 and normal levels of ASPP and certain leukemias, underlining its potential importance in cancer (Zhang at al., 2005). Apoptosis inhibition can be important in carcinogenesis and disease progression. Thus, if PPP1R13L has an anti-apoptotic role it might play role as an oncogene; in contrast if it is pro-apoptotic it might act as tumor suppressor. Some data suggest PPP1R13L is over or underexpressed under certain experimental settings, consistent with both possibilities. We speculated that PPP1R13L can function as an oncoprotein, and that establishment and maintenance of tumors would be modulated by PPP1R13L. Therefore, to study the role of PPP1R13L in tumorigenesis we have used a combined in vitro and in vivo strategy. We have used primary mouse embryonic fibroblasts (MEF's) as a model system. MEF's expressing adenovirus E1A and activated ras undergo p53-dependent apoptosis when treated with DNA-damaging or chemotherapeutic agents such as doxorubicin (Adriamycin), etoposide (Lowe at al., 1993). They also rapidly form tumors in nude mice. Utilizing these strategies we have explored the effects of PPP1R13L expression on dually transformed cells differing in their p53 status to examine the ability of PPP1R13L to act as an oncoprotein. Indeed, we found that over-expression of PPP1R13L strongly accelerated tumor formation by ras/E1A transformed cells and gave a phenotype with multiple tumor nodes, consistent with increased metastasis. At the same time the PPP1R13L over-expressing cells seemed depleted for both p53 and active p65/RelA. Through several different lines of investigation, we provide evidence that both p53 dependent and independent apoptosis pathways are regulated by PPP1R13L. Finally, studies with the proteasome inhibitor MG132, suggest that over-expression of PPP1R13L causes faster p53 degradation, a likely explanation for the depletion of p53. The combined results indicate that over-expression of PPP1R13L will accelerate tumor growth and may be important for tumor metastasis.

RESULTS

PPP1R13L suppresses apoptosis induced by multiple stimuli in E1A/ras transformed mouse embryonic fibroblasts.

p53 is required for the efficient activation of apoptosis following treatment with chemotherapeutic compounds (Lowe et al., 1993), and absence of p53 expression leads to a dramatic increase in cellular resistance to these agents. The hypothesis that the PPP1R13L protein is an inhibitor of the p53 tumour suppressor, and that its expression enhances growth and tumorigenic potential of ras/E1A expressing MEFs, led us to examine the effect of various anticancer agents on ras/E1A transformed fibroblasts lines over-expressing PPP1R13L protein. We characterized the apoptotic response of wild-type and p53 null ras/E1A MEFs expressing PPP1R13L or control vector infected cells to doxorubicin and Etoposide, 24 after treatment using doses that have previously been reported to induce apoptosis in E1A, ras-expressing MEFs (Lowe et al., 1993) **(Figure 1)** shows a representative experiment of a series of 4 experiments in total. Doxorubicin and Etoposide efficiently induced apoptosis in ras/E1A wild-type MEFs but not in p53-null ras/E1A MEFs. Overexpression of PPP1R13L inhibited apoptosis induced by both compounds in MEFs ras/E1A which are wild type for p53 gene. Expression of PPP1R13L in cells, which were null with respect to p53, had very little effect.

PPP1R13L does not influence cell cycle progression in E1A/ras transformed mouse embryonic fibroblasts.

We examined whether PPP1R13L overexpression has any effect on cell cycle progression in studied cell lines. FACS based cell-cycle analysis revealed in no significant differences between ras/E1A transduced MEFs, and their PPP1R13L expressing counterparts **(Figure**

2a). Further, we confirmed these results by protein expression blotting for cyclines, which are involved in the progression of cells through the cell cycle **(Figure 2b)**. No differences in the protein levels for cyclin A, CDK4, cyclin D were observed between ras/E1a transduced MEFs and their PPP1R13L overexpressing parallel lines. Taken together our results show that PPP1R13L overexpression inhibits p53 dependent apoptosis but has no effect on cell cycle progression in ras/E1A transduced mouse embryonic fibroblasts.

PPP1R13L enhances transformation in vitro in a manner that is largely p53-dependent.

Transformation of cells with a combination of oncogenic H-ras and Adenovirus E1A is a well established way to obtain genetically defined malignant cells. Transformation through oncogenic ras requires either a cooperating oncogene or the inactivation of a tumour suppressor to abrogate senescence. The adenovirus E1A oncogene serves this function.

To explore the role of gene PPP1R13L function and its interactions with the p53-tumour suppressor gene in a model of cancer progression, we used transformed embryonic fibroblasts obtained from knockout p53 -/- mice and their wild type counterparts. Specifically, we were interested whether over-expression of the PPP1R13L protein could modulate ras/E1A mediated transformation. Therefore, p53 -/- and wild-type MEFs were infected with a retroviral vector overexpressing both ras and /E1A retroviral vector (which co-expressed H-rasV12 together with the adenovirus E1A 12S oncogene) and a retroviral vector expressing the PPP1R13L protein, to obtain transformed fibroblasts with defined p53 and PPP1R13L status. Cells infected with the respective empty retroviral vectors were used as a negative control. We evaluated the effect of the oncogenes by examining changes in the morphological aspects (i.e. cells lost their flat and enlarged cytoplasm and became retractile with thin projections).

To characterize these cell populations, we quantified expression of the PPP1R13L mRNA and protein by qPCR and western blot, and monitored cell proliferation. Retroviral transduction increased the PPP1R13L mRNA expression about 100 fold and the protein expression approximately 3 fold compared to endogenous levels **(Supplementary figure 1).** We next plated PPP1R13L-expressing p53-wildtype ras/E1A MEFs cells and wild-type ras/E1A control MEFs at low density and examined colony formation. PPP1R13L-expressing p53-wildtype ras/E1A MEFs cells grew significantly faster and formed more colonies than their control counterparts when plated at low density, but not quite as fast as the p53-null cells. Importantly, PPP1R13L-expressing, oncogene-transduced MEFs, which were null for p53 tumour suppressor gene also formed more colonies as compared to p53 null ras/E1A MEFs control cells **(Figure 3a and 3b).**

The same infected mouse embryo cultures were also tested for their ability to form colonies in soft agar **(Figure 3b).** Wild type MEFs and p53 -/- MEFs transduced with both E1A and ras formed anchorage-independent colonies, but with different efficiencies. In marked contrast to ras/E1A transformed MEFs, those additionally over-expressing PPP1R13L formed 2-3 fold more colonies in soft agarose. Similarly to results obtained from colony formation assay, ras/E1A transduced MEF's null for p53 but over-expressing PPP1R13L also formed a greater number of agar foci. Thus, PPP1R13L was identified as a novel oncogene that cooperates with Ras and E1A to transform cells in vitro. These results support the hypothesis that one mechanism by which PPP1R13L potentiates the transforming activity of ras/E1A oncogenes is through its ability to inactivate p53 tumor suppressor gene, but the data further suggest that PPP1R13L also acts as an oncogene in a p53- independent manner.

PPP1R13L promotes p53 turnover.

We and others have previously reported that PPP1R13L expression decreases p53 protein expression levels and that PPP1R13L expression regulates p53-mediated apoptosis (Lu Xin et. al, 2003.). PPP1R13L also inhibits p53 transcriptional activity in luciferase reporter assay (data not shown), thus confirming that primary role of PPP1R13L is to inhibit pro-apoptotic activity of p53 that is normally stimulated in response to genotoxic stress We were interested whether PPP1R13L expression regulated p53 stability and proteasomal degradation of p53. Indeed, we found this to be the case **(Figure 4).** The degradation could be blocked by the proteasome inhibitor MG132. Wild-type ras/E1A transduced cells with or without PPP1R13L, were incubated with or without MG132 and after indicated time level of p53 was determined. We observed a dramatic pile-up of p53 in the PPP1R13L-overexpressing, MG132-treated cells, consistent with the notion that p53 is rapidly degraded by proteasome in PPP1R13L-overexpressing cells. Although the mechanism whereby this occurs remains to be determined, it is noteworthy that PPP1R13L belongs to a group of proteins, acting as a “targeting proteins”, i.e. facilitating the binding catalytic units of proteins to their targets. Thus, PPP1R13L may act by guiding a catalytic unit involved in protein modification to its presumptive targets. The consequences of the modification may well be the degradation of the target, i.e. p53.

In vivo, PPP1R13L promotes tumorigenesis through both p53- dependent and independent mechanism.

p53 tumor suppressor activity has been extensively studied in primary rodent cells, where p53 mutations can cooperate with the combinations of ras and E1A oncogenes, in promoting oncogenic transformation (Lowe et al., 1994). Reduction of apoptosis provides a mechanism for this effect (Hemann PNAS 2005). We therefore investigated whether reduced susceptibility to apoptosis due to PPP1R13L overexpression would increase tumorigenic potential. To determine the extend which PPP1R13L overexpression could mimic p53 function in this assays; we used cells harboring the same genetic lesions as described above to induce tumors in the rear flanks of immunocompromised mice.

After retroviral infection, cell populations were injected s.c into nude mice and mice were continuously monitored for tumor formation at the sites of injection **(Figure 5).** Of note, all studied cell lines expressed equivalent high levels of ras and E1A as estimated by Western blot analysis **(supplementary material Figure 1**). Consistent with previous studies that E1A and ras are sufficient for tumorigenic conversion of wild-type MEFs, tumor formed in animals injected with these cells within 20-30 days. E1A and ras were also sufficient to cause tumorigenic conversion in p53-null MEFs, with the tumors forming after 10-20 days. Importantly, in all cases tumors formed faster in animals injected with PPP1R13L expressing cells. p53 - wild type, PPP1R13L overexpressing ras/E1A cells were highly tumorigenic, with latency periods similar to p53-/- cells coexpressing ras and E1A.

ras/E1A PPP1R13L p53-null MEFs also developed tumors faster than ras/E1A p53-/- MEFs. ras/E1A PPP1R13L p53-null MEFs developed bigger solitary tumors in all nude mice than ras/E1A p53-/- MEFs **(Figure 5).** Strikingly, ras/E1A PPP1R13L expressing p53-wildtype MEF’s developed aggressive subcutaneous tumors with local satellite tumors and also more distant metastasis in some cases. Notably, this phenotype was not seen in the absence of p53. Nevertheless, these results are in agreement with our in vitro results and support the idea that PPP1R13L plays a role in tumorigenesis and progression. Histopathological evaluation revealed that the developing tumors could be classified as aggressive sarcomas with a high proliferation rate as assessed by the frequency of mitotic figures **(Figure 6a and b).**

Explanted tumors cells retain their in vitro phenotypes.

The growth curves **(Figure 7a)** show that in ex-vivo cells that are p53-wildtype, PPP1R13L overexpression caused the cells to grow faster. The grow kinetics was similar to p53-/- ras/E1A MEFs colonies. Western blot probing confirmed that each cell lines expressed ras, E1A protein, and where indicated PPP1R13L protein **(Figure 7b).** PPP1R13L suppressed apoptosis induced by multiple stimuli (doxorubicin, etoposide) in tumor derived clones, which respond to treatment, the same way as original clones. This indicates that tumorigenicity did not result from additional mutations that might suppress apoptosis. In all experiments and under all tested conditions cells expressing PPP1R13L protein showed markedly higher viability, whether or not they were wild-type or p53 null **(Figure 8**).

To further confirm this observation we explored the use of the active form of caspase-3 for the detection of apoptotic event. Fluorescence images **(Figure 9)** for PPP1R13L expressing cell, showed very few positive cells for activated caspase-3 in response to the apoptosis-inducing drug doxorubicin. In the case of p53 null ras/E1A PPP1R13L transduced clones almost no staining could be detected indicating high resistance of those cell to the above mentioned treatments. Additionally, no difference in BrdU incorporation could be detected between wild-type ras/E1A, p53-/- ras/E1A transduced cells and the paired PPP1R13L expressing cells **(Figure 1**0). Thus, PPP1R13L expression in tumor derived cells conferred cellular resistance to the cytotoxic effect of doxorubicin and etoposide.

PPP1R13L promotes cell migration and modulates p53-dependent cell death in suspension.

Enhanced cell migration is often a characteristic of invasive tumor cells (Nikiforov et al., 1996). Based on our demonstration that the PPP1R13L overexpressing wild-type tumors had a distinct phenotype we examined the effects of PPP1R13L modulation on migration. We used stably clones of wild-type ras/E1A and p53-null ras/E1A MEFs with/or without PPP1R13L. We tested the ability of the cells to migrate in a wound-healing assay. Cells were physically removed from a confluent monolayer and the ability of cells to fill the available space was quantified using phase-contrast microscopy. After 24 hours, the p53 -/- ras/E1A transduced cells with or without PPP1R13L closed the wound completely. In comparison, the p53-wildtype PPP1R13L expressing transduced cells, moved significantly towards the gap, whereas wild type ras/E1a control cells almost failed to migrate **(Figure 11).** For phase contrast microscopy images see **(Supplementary Figure 2)**. It has been shown that p53 promotes apoptosis in ras/E1A transformed MEF's detached from substrate which could eliminate disseminated cells in vivo in the bloodstream (Nikiforov et al., 1996). To determine whether PPP1R13L expression might influence cell viability following disruption of cell-substrate interactions, we examined the viability of ras/E1A transformed MEF's with known p53 and/or PPP1R13L status. Cell viability in floating assays and in methylcellulose was determined as illustrated in **(Figure 12a and b).** ras/E1A transduced p53 null MEF's expressing PPP1R13L/vector control showed no significant reduction in viability after 24h in suspension. These cells kept growing in suspension as if they were on solid substrate. However wild-type ras/E1A MEF's when incubated in suspension showed a dramatic decrease in cell viability. Thus, the rapid cell death of wild-type ras/E1a transformed MEF's can be partially prevented by PPP1R13L over-expression. To further confirm our findings, we have also studied cell survival in methylcellulose **(Figure 12b).** Again, survival rate of wild-type ras/E1A transduced cells expressing PPP1R13L was strongly stimulated as compared to control cells (wild-type ras/E1A). This increase in cell viability after incubation in methylcellulose was p53 dependent, since p53 null ras/E1A MEF's expressing PPP1R13L/vector control did not exhibit significantly altered cell growth. We conclude that in wild-type ras/E1A transformed MEF's, abrogation of p53 dependent apoptosis by PPP1R13L over-expression promotes the survival of cells detached from substrate.

Discussion

In the present work, we have used ras/E1A transformed mouse embryo fibroblasts (MEFs) as a model of tumour formation to analyze the role of PPP1R13L in tumour establishment and progression. This model was chosen because transformation is induced in a simple and controlled way, avoiding the difficulties of analyzing the multiple and complex transformation mechanisms observed in cellular models derived from human tumors.

Suppression of apoptosis is an integral part of the oncogenic transformation process (Lowe et al., 1994). E1A expression induces an abortive transformation, but also induces p53 accumulation, which in turn accelerates apoptosis (Lowe and Ruley, 1993; Samuelson and Lowe, 1997). Therefore, E1A alone can transform p53-deficient, but not normal p53-expressing, primary mouse embryonic fibroblasts (Lowe et al., 1994). Conversely, previous studies have reported that oncogenically activated H-ras rescue cells from p53-dependent apoptosis, but H-ras is unable to relieve the growth suppression induced by p53 (HJ Lin et al., 1995). Thus, on their own, neither E1A nor H-ras are capable of promoting sustained cell proliferation, whereas E1A and H-ras together blocks apoptosis, relieves growth arrest and as a consequence promotes oncogenic transformation. The cooperation between the two oncogenes provides sufficient complementary growth-stimulatory signals (HJ Lin et al., 1995). In the present study our observations were made using both transformed p53 wild-type and transformed p53 null MEF's making it possible to evaluate the role of p53 in the cells.

qPCR results showed that the level of mRNA encoding PPP1R13L protein increased about hundred fold after transfection. In contrast, the level of PPP1R13L protein was only moderately increased. This apparent discrepancy was most likely due to fast turnover of the synthesized protein. This became apparent when degradation was blocked by the proteasome inhibitor MG132 and PPP1R13L accumulated to high levels.

Transfection with the PPP1R13L encoding vector led to depletion of active p65/RelA and p53 in the p53-wildtype cells. In the p53 null cells active p65/RelA was not eliminated. It is not clear how p53 contributed to elimination of NF-κB. Again, the elimination seemed associated with rapid degradation, as the proteins piled up in cells treated with MG132. As it is known that PPP1R13L binds to these proteins, one can speculate that PPP1R13L-binding targets them for proteasome degradation.

In agreement with previously published results (Bergamaschi et al., 2003), PPP1R13L-overexpressing cells were significantly more resistant to undergo an apoptosis process. We have found no changes in cell cycle progression of cells. In conclusion, PPP1R13L is a potent p53 inhibitor, and inhibits apoptosis, but has no affect on cell-cycle arrest.

When we studied cell transformation with in vitro techniques it became apparent that transfection of wt p53 cells with the PPP1R13L-encoding vector led to a more transformed phenotype, reminiscent of that of the p53 null cells. This was true for assays of cloning efficiency, soft agar growth and cell migration, all assays reflecting aspects of a transformed phenotype. The transfection had a limited effect on the p53 null cells in these assays.

Our in vivo results demonstrated that the latency of tumors in nude mice was diminished and size was increased by transfection with the PPP1R13L encoding vector. In the case of p53 wild-type MEFs stably over-expressing PPP1R13L, we also observed a very characteristic “multifocal” phenotype, not observed in other settings. This phenotype suggests that the malignant cells migrated with greater ease in the animal. After injection of cells devoid of p53, those over-expressing of PPP1R13L produced tumors of greatly increased size, but the phenotype was still a solitary tumor.

Ex vivo studies indicated that the cell properties had not been changed during tumor growth. Thus, the in vivo studies allowed us to distinguish between absence of p53 and overexpression of PPP1R13L, and in particular the effect in p53 null cells indicated that PPP1R13L must have other targets than p53. NF-κB was only depleted in p53 wild type cells and one possibility is that depletion of p65/RelA led to the unusual multifocal phenotype in the p53 wild-type cells, but other targets for PPP1R13L could also cause this effect. We note with interest that Ryan et al have reported that loss of p65/RelA in these transformed cells accentuates their transformed character, but does not simulate the loss of p53 (Ryan et al., 2004). The multifocal phenotype could again reflect increased tumor migration and/or metastasis, a possibility that we currently pursue.

To our knowledge, this study represents the first report that PPP1R13L functions as an oncoprotein, using both in vitro and in vivo approaches. However, PPP1R13l previously showed an ability to inhibit p53-mediated apoptosis in response to DNA damage in two human cell lines; U2OS and MCF7 (Bergamaschi et al., 2003). Also, our findings are consistent with an early observation that the apoptotic, but not cell-cycle-arrest function of p53 is required to suppress the transforming activities of ras and E1A (Ludwig et al., 1996).

There are two caveats with our experiments; First, the experiments deal with the expression of human PPP1R13L in mouse cells. Thus one must consider the possibility that species differences influence the results. We think this unlikely as PPP1R13L is known to be a highly conserved protein (Bergamaschi et al, 2003). Secondly, the experiments deal exclusively with over-expression of PPP1R13L under the control of an external promoter without the putative regulation of the endogenous counterpart. Also, the experiments focus on transformed cells only. Thus, our experiments deal with the function of PPP1R13L in the context of a malignant setting and shed little light on its normo-physiological role.

Although previous reports have suggest that PPP1R13L can function as an oncoprotein (Bergamaschi et al, 2003), (A Sullivan and X Lu, 2007), we now provide a combination of in vitro and in vivo techniques to directly support this contention. Moreover, the finding that PPP1R13L can stimulate cell migration and metastasis though p53-independent mechanisms is surprising, and extend the interest in this protein beyond simply its anti-apoptotic activity. How this occurs remains to be determined, but it is clear that PPP1R13L can signal through multiple targets. In principle, its ability to signal through distinct mechanisms may explain its different actions in the cell.

Supplementary information is available at Oncogene’s website.

Materials and Methods:

Cells, Plasmids and Gene transfer.

WT and p53 -/- mouse embryonic fibroblasts (MEF's) were cultured in Dulbecco's modified Eagle's medium containing 10% fetal bovine serum (FBS) and used between passages 3 and 5. Retroviral vectors were as follows: LPC, control vector expressing puromycin phosphotransferase (*puro*). Control CyclineD pLPC, a human cycline D cDNA in pLPC puro. *RAI* pLPC (kindly donated by Kevin M. Ryan, Beatson Institute for Cancer Research, Glasgow, United Kingdom) was cloned into PCB6$^+$ from cDNA with primers containing KpnI and NotI restriction sites. An EcoRI/EcoRV fragment from plasmid was then cloned into pLPC to generate *RAI* pLPC vector. Oncogenic *ras* (H-*RasV12)* and *E1A* were expressed by using WZL-Hygro-based retroviral vectors. *E1A/H-RasV12* was expressed by using a modified pBabe H-RasV12 retroviral vector. Retroviruses were generated by transfection of Phoenix packaging cells (G. Nolan, Stanford University, Stanford, California, USA). Infective supernatants were then administered to target cells followed by appropriate drug selection, puromycin (2µg/ml, 2 days) or hygromycine (75 µg /ml, 3days). Calcium phosphate precipitation was used to transiently transfect cells.

Colony Formation assay and Soft Agar Transformation Assay

For in vitro colony formation assay five thousand cells were plated in 60-mm dishes in complete culture medium. Triplicate experiments were performed for each cell clone. The medium was changed on cells every 4 days. On the 10th day, plates were fixed with 4% formaldehyde, washed twice, and stained with 1% crystal violet, and the colonies were quantified. For soft agar transformation assays, cells were resuspended in 0.3% Noble agar (in DMEM supplemented with 10% FBS) at a density of 2x 10^4 cells per well (in six-well plates), and were plated onto solidified 0.5% Noble agar-containing bottom layer medium.

Plated cells were fed weekly and were incubated at 37^0c for 21 days. Plates were stained with 0.005% crystal violet for 1h. Colonies were counted under a dissecting microscope. Experiments were repeated twice, and MEFs from two different infections were used in each assay.

BrdU incorporation and DNA content analysis

For BrdU incorporation and DNA-content analysis, subconfluent cultures were labeled with 10µM BrdU (Amersham) for 6h. Cells were trypsinized and fixed in 75% ethanol for 30 min. Cells were washed in PBS and were treated subsequently with 2 M HCL for 20 min at room temperature. After washing in washing buffer (0.1% BSA/PBS), cells were neutralized in 0.1 M sodium borate for 2 min followed by washing in washing buffer. Cells were incubated subsequently with FITC-conjugated anti-BrdU antibody (Pharmingen) for 1h at room temperature. Finally, cells were washed in washing buffer three times followed by treatment with propidium iodide (10 µg/ml) and RNase A (100 µg/ml) at 37^0C for 30 min. Samples were analyzed by Flow Cytometry.

Cell viability and apoptosis

Cells were plated in 96-well plates ($2x10^4$ cells per well) or 10cm- culture dishes at concentration 7, 5 x 10^5 cells per plate. 24h after plating cells were washed and medium was replaced with culture medium containing appropriate drug at indicated concentrations. After drug addition cells were incubated for indicated time periods. Cell viability was measured using CellTiter-Blue ® Cell Viability Assay according to the protocol provided by the manufacture. Cells growing on 10cm culture plates were stained with fluorescein isothiocyanate (FITC)-annexin V. Staining with FITC-annexin V and propidium iodide were performed according to the manufacture instructions (BD Pharmingen). Cells were analyzed by Flow Cytometry.

Western Blotting

Whole-cell lysates were derived by lysing cell pellets in SDS sample buffer (60mM Tris-HCl at pH 6.8, 10% glycerol, 2% SDS, 5% 2-mercaptoethanol). Samples corresponding to 30µg of protein (Bio-Rad protein assay) were separated on SDS-PAGE gels and transferred to Immobilon-P-membranes (Millipore). The primary antibodies used were as follows: Anti-p53 polyclonal antibody (CM5, or 505, 1:1000, NovaCastra,), anti-H-Ras antibody (C-20, sc-520, 1:1000 Santa Cruz Biotechnology), anti-E1A antibody (sc-430 (13S-5) 1:500, Santa Cruz Biotechnology), anti-RAI (1; 500, Sigma Aldrich), anti- cycline A antibody (c-19, 1:1000 Santa Cruz Biotechnology), anti- cdk4 antibody (c-22, 1:500 Santa Cruz Biotechnology), anti-cycline D (c-20 1.1 1:1000 Santa Cruz Biotechnology), anti-phospho NF-kappaB p65 antibody (1:1000 Santa Cruz Biotechnology), and anti-Tubulin antibody (1:1000 Abcam).

Immunofluorescence

Cells growing at a confluence of 50% on coverslips in 6-well plates were treated with indicated drugs and for indicated period of times. At the end of treatment, cells were fixed in 3.7% formaldehyde in PBS followed by a 5 min permeabilization in 0.1% Triton X-100 in PBS and were incubated in PBS containing 0.1% BSA before staining with primary antibody. For caspase-3 expression, anti-cleaved caspase 3 monoclonal Antibody (1:1000, R&D Systems) was used. Subsequently slides were counterstained with DAPI and analyzed under fluorescence microscopy. Cells were quantified by averaging 3 optical fields under 40 x magnifications on 2 slides from 2 independent experiments.

Tumorigenicity Assays

To measure the tumorigenic potential of the different MEF cultures, cells were injected in to athymic mice. Four-to 6-week old nude mice were obtained from Cold Spring Harbor

Laboratory and maintained in the animal facility building at Cold Spring Harbor Laboratory in accordance with the institutional guidelines. Animals were kept in numbers no greater that 5/cage and had unlimited access to food and water. A total of 1.5×10^6 cells from each of the MEF cultures were suspended in PBS and injected s.c. into each flank of an animal, with 4 animals being used for each cell line. After injection, mice were monitored three times/week for tumor formation. Once, apparent, the tumors were measured with calipers, and tumor volume was calculated using following formula: tumor volume (mm^3) as length $\times \text{width}^2 \times \pi/6$. Animals with tumor measuring in excess of 1200 mm^3 were sacrificed. For analysis of protein expression, tumors were snap-froze and pulverized in liquid nitrogen using a mortar and pestle. For western blotting powdered tumors were lysed in Laemmli buffer. For histology analysis, tumors were fixed for 16h in 4% formalin in PBS before embedding and sectioning. The Cold Spring Harbor Laboratory Animal Care and Use Committee approved all mouse experiments described in this work.

Histopathology

Fixed tissue samples were embedded in paraffin, and sections (7μm) were stained with hematoxylin and eosin (H&E) according to standard protocols. For detection of KI67, representative sections were deparaffinized, rehydrated and processed in graded alcohols using the avidin-biotin immunoperoxidase method. Briefly, sections were submitted to antigen retrieval by microwave oven treatment for 15 min in TRYLOGY buffer. First, slides were incubated in 10% normal goat serum for 30 min and then overnight at 4^0 C with appropriate diluted primary antibody (rabbit antibody against Ki67, NovoCastra). Next, slides were incubated with biotinylated goat rabbit-specific immunoglobulins (Vector Laboratories) at 1:500 dilution for 30 min and then with avidin-biotin peroxidase complexes (1:25; Vector Laboratories) for 30 min. As a chromogen, diaminobenzidine was used, and hematoxylin as the nuclear counterstained. Histopathological evaluation of carcinomas was performed by an experienced pathologist (L.Z) using paraffin embedded tumor sections stained with Hematoxylin/Eosin.

Wound Healing Assay

Cell migration was measured using *in vitro* wound healing assay. Briefly, *in vitro* "scratch" wounds were created by scraping confluent cell monolayers in Petri dishes with a sterile pipette tip. After 24h incubation in DMEM with 0,5% serum, migration was quantified by counting cells migration distance from the wound edge. Phase contrast microscopy images were taken using Axioskop (Zeiss), at 40x magnification. Each determination represents the mean of 5 measurements from at least two individual experiments.

Assays for cell survival in suspension and cell growth in methylcellulose

Both assays were performed according to previously published protocols (Nikiforov MA, et al. 1996).

Proteosome inhibition

Unless otherwise noted, WT ras/E1A PPP1R13L/vector control and p53-/- ras/E1A PPP1R13L/vector control cells were treated prior to collection with 100µM MG132 (Sigma Aldrich) for 4h. Cells were washed with PBS and subsequently lysed for 30 minutes at 4^0C in a buffer containing 120 mM NaCl, 50 mM HEPES pH 7.2, 1mM EDTA, 0,1% NP-40, and Complete protease inhibitor cocktail (Roche). Protein concentration was determined using (Bio-Rad protein assay). Samples were separated on SDS-PAGE gels and transferred to Immobilon-P-membranes (Millipore). The primary antibodies used were as follows: Anti-p53 polyclonal antibody (CM5, or 505, 1:1000, NovaCastra,), anti human PPP1R13L antibody (Invitrogen 1:1000),anti-phospho RelA-p65 antibody (Santa Cruz 1:1000) and anti-Tubulin antibody (1:1000 Abcam).

Acknowledgements

We thank Kevin Ryan for providing necessary vectors. We are grateful to Pamela Moody for helping with FACS analysis, and Katherine McJunkin for assistance with in vivo assays.

References

1. Bergamaschi D, Samuels-Lev Y, Jin B, Duraisingham S, Crook T, and Lu X. (2004). ASPP1 and ASPP2: common activators of p53 family members. *Mol. Cell. Biol.* 24, 1341-1350.
2. Bergamaschi D, Samuels-Lev Y, O'Neil NJ, Trigiante G, Crook T, Hsieh JK, et al. (2003). iASPP oncoprotein is a key inhibitor of p53 conserved from worm to human. *Nature Genet.* 33, 162-167.
3. Laska MJ, Strandbygard D, Kjeldgard A, Mains M, Corydon T, Memon A. (2007). Expression of the RAI gene is conductive to apoptosis: Studies of induction and interference. *Exp Cell Res.* 15, 2611-2621.
4. Lin HJ, Eviner V, Prendergast GC and White E. (1995). Activated H-ras rescues E1A-induced apoptosis and cooperates with E1A to overcome p53-dependent growth arrest. *Mol.Cell.Bio.,* 4536-4544.

5. Lowe SW, Ruley HE. (1993). Stabilization of the p53 tumor suppressor is induced by adenovirus-5 E1A and accompanies apoptosis. *Genes Dev.* 7, 535-545.
6. Lowe SW, Ruley HE, Jacks T, and Housman DE. (1993). P53-Dependent Apoptosis Modulates the Cytotoxicity of Anticancer Agents. *Cell.*74, 957-967.
7. Lowe SW, Jacks T, Housman DE, Ruley HE. (1994). Abrogation of oncogene-associated apoptosis allows transformation of p53-deficient cells. *Proc Natl Acad Sci USA.* 91(6), 2026-2030.
8. Ludwig RL, Bates S, and Vousden KH. (1996). Differential activation of target cellular promotes by p53 mutants with impaired apoptotic function. *Mol. Cell. Biol.* 16, 4952-4960.

9. Nikiforov MA, Hagen K, Ossovskaya VS, Connor T, Lowe SW, Deichman GI, et al. (1996). P53 modulation of anchorage independent growth and experimental metastasis. *Oncogene*. 13,1709-1719.
10. Nikiforov MA, Kwek S, Mehta R, Artwohl JE, Lowe SW, Gupta TD, et al. *Onocgene*. 15, 3007-3012.

11. Ryan KM, O'Prey J and Vousden KH. (2004). Loss of Nuclear Factor-κB Is Tumor Promoting but Does Not Substitute for Loss of p53. *Cancer Research* 4415-4418.
12. Samuels-Lev Y, O'Connor DJ, Bergamaschi D, Trigiante G, Hsieh JK, Zhong S, et al,. (2001). ASPP proteins specifically stimulate the apoptotic function of p53. *Mol. Cell*, 8, 781-794.
13. Samuelson AV, Lowe SW. (1997). Selective induction of p53 and chemosensitivity in RB-deficient cell by E1A mutants unable to bind RB-related proteins. *Proc. Natl. Acad. Sci. USA* 94, 12094-12099.
14. Slee EA and Lu X. (2003). The ASPP family: deciding between life and death after DNA damage. *Toxicol. Letters*, 139, 81-87.
15. Sullivan A, and Lu x. (2007). ASPP: a new family of oncogenes and tumour suppressor genes. *Cancer Research UK.* 96, 196-200.
16. Trigiante G, and Lu X. (2006). The ASPPs and cancer. *Nature Rev.Cancer,*6, 217-226.

17. Yang JP, Hori m, Sandra T, and Okamoto T. (1999). Identification of a novel inhibitor of nuclear factor-kappaB, RelA-associated inhibitor. *J. Biol. Chem.* 24, 15662-15670.

18. Zhang Z, Wang M, Zhou C, Chen S, Wang J. (2005). The expression of iASPP in acute leukemias. *Leuk Res.* 29, 179-183.

Titles and legends to figures.

Figure 1

PPP1R13L suppresses apoptosis induced by multiple stimuli in E1A/ras transformed MEF’s.

Cultures of ras/E1A transformed wild-type or p53 -/- MEF’s, expressing PPP1R13L or vector alone were treated with the compounds indicated for 24h *(see materials and methods).* Cells, both adherent and floating, where then harvested and analyzed by flow cytometry. The percentage of cells with sub-G1 content was taken as a measurement of apoptotic rate. Similar results were obtained when cells were stained with Annexin-V fluorescence dye and analyzed by flow cytometry.

Figure 2

PPP1R13L does not influence cell cycle progression in E1a/ras transformed MEF’s.

a) Cell cycle analysis of ras/E1A transformed wild-type and p53 -/- MEF’s, expressing PPP1R13L or vector alone. Histogram of all cell cycle phases for all studied cell lines. Data are presented as the average ± SD from three independent experiments.

b) Western Blot analysis for cyclines controlling cell cycle progression. Western blot analysis of cyclin A, cdk4, cyclin D in ras/E1A transformed wild-type and p53-/- MEF’s expressing PPP1R13L or vector control. Tubulin level is shown as a loading control. Cdk4- cyclin-dependent kinase 4.

Figure 3

PPP1R13L enhances transformation *in vitro* in a manner that is largely p53-dependent.

a) Colony formation assays on wild-type and p53 null MEF's infected with viruses carrying PPP1R13L or vector alone. Cells were plated at equal densities, cultured in the presence of selective antibiotics for 10-15 days, fixed and stained with crystal violet.

b) Quantification of colony formation assays. Colony numbers were estimated ~ 2 weeks after transfection and represent the average ± SD determined from at least three transfections. Soft agar assays. Cells expressing indicated gene combinations were plated in soft agar media and growth was monitored. Colonies were scored after 3 weeks. Data represents the average ± SD determined from at least three independent experiments.

Figure 4

PPP1R13L promotes p53 turnover.

For p53 degradation Ras/E1A transduced wild type MEF's expressing PPP1R13L/vector control were incubated with proteasome inhibitor 100μM MG132 for 4h. Lysates were prepared as described in Materials and Methods, and subjected for Western Blotting with anti-p53 antibody. For PPP1R13L and RelA p65, proteasomal degradation ras/E1A transduced wild type and p53 null MEF's were incubated for 4h with 100μM MG132 inhibitor and treated as above. Membrane was probe with anti-PPP1R13L antibody and anti-phospho p65antibody . Tubulin is shown as a loading control.

Figure 5

***In vivo*, PPP1R13L promotes tumorigenesis through both p53-dependent and independent mechanism.**

In vivo tumor growth. Ras/E1A-transformed wild-type or p53 -/- MEFs of the indicated PPP1R13L genotypes (retroviral vector carrying PPP1R13L or only vector control) were injected into both flanks of athymic nude mice. Animals were checked periodically for tumor formation, and the dimensions of tumors were measured three times a week with calipers. Tumor size is plotted as tumor volume over time. Representative image showing characteristic "bubbly" phenotype of wild-type ras/E1A -PPP1R13L driven tumors.

Figure 6

Tumors examinations.

- **a)** Haematoxylin and eosin (H&E) immunohistochemical staining. Histology of surgical resections showing malignant cells with numerous mitotic figures in a desmoplastic background. Tumor tissues stained for proliferating activity with KI-67.
- **b)** Quantification of high incidence of mitotic cells in histological section of tumors. Data represents average ± S.D from three independent tumor sections. From each slide of each tumor at least 6 pictures were acquired and cells well counted.

Figure 7

Explanted tumors cells retain their *in vitro* phenotypes.

- **a)** Ex-vivo growth characteristics of ras/E1A transduced, wild-type and p53-/- cells expressing PPP1R13L or vector alone control. Cells were plated in 6 cm dishes at the density of $1x10^5$/dish. Cells were then counted every day for 7 days. The results shown are derived from at least three independent experiments for each time point.

b) Cell extracts were prepared from cell cultured ex-vivo from tumor mass and were subjected to Western blotting with the indicated antibodies. Tubulin served as a loading control.

Figure 8

Explanted tumors cells retain their *in vitro* phenotypes.

Cultures of ras/E1A transduced, PPP1R13L/vector control expressing, wild-type and p53-/- cells, were treated with indicated compounds at indicated concentration for 24h. Cell viability was assessed using CellTiter-Blue™ cell viability assay. The results shown are derived from at least three independent experiments for each treatment and each tested concentration.

Figure 9

Explanted tumors retain their *in vitro* phenotypes.

Immunofluorescence staining of caspase 3 in ex-vivo cultured cells using antibody against activated caspase 3. Cells were treated for 24h with 200ng/ml Adriamycin. The red signal represents staining of cleaved/activated caspase 3, counterstaining with DAPI is shown in blue.

Figure 10

Explanted tumors cells retain their *in vitro* phenotypes.

BrdU incorporation for 8h of ras/E1a transduced PPP1R13L/ vector control expressing, wild-type and p53 -/- cells. BrdU incorporation visualized by ant-BrdU immuonoflurescence (red) and co-stained with DAPI (blue).

Figure 11

PPP1R13L promotes cell migration.

Scratch wound assay on studied cells populations grown until confluence and on which a “mechanical” wound had been made. Quantitative determination (computer assisted phase contrast microscopy) of the ability of wild type ras/E1A and p53 null ras/E1A cells expressing PPP1R13L/vector control, to recolonize the wound. For phase contrast microscopy images see supplementary materials (Figure 2). The data are given as the means of 5 measurements from at least two independent experiments ±SEM.

Figure 12

PPP1R13L modulates p53-dependent cell death in suspension.

a) Comparison of viability of different cell types in suspension. Cell quantification was done by MTT assay and/or CellTiter-Blue™ cell viability assay in 4h after plating cells subjected to 24h floating. All values were normalized to the values obtained in control cells growing 4h on plate. Closed bars –viability of control cells, color bars-viability of cells after 24h of floating.

b) Dynamics of the decrease in viability of cells subjected to incubation in methylcellulose. All values were normalized to the values obtained in control cells growing on plate for corresponding time intervals. Cell quantification was done by MTT assay and/or CellTiter-Blue™ cell viability assay.

Supplementary materials

Figure 1 In vitro Western blotting.

Lysates were prepared from wild-type and p53-/- ras/E1A transformed MEFs expressing PPP1R13L/vector control and analyzed for expression of indicated proteins. Antibodies used were; -H-Ras antibody (C-20, sc-520, 1:1000 Santa Cruz Biotechnology), anti-E1A antibody (sc-430 (13S-5) 1:500, Santa Cruz Biotechnology), anti-RAI (1; 500, Sigma Aldrich). Tubulin is shown as a loading control.

Figure 2 In vitro wound healing assay

Phase contrast images from wound healing assays. Cells were treated as described in materials and methods. Images were acquired using Axioskop Zeiss at magnification 40x.

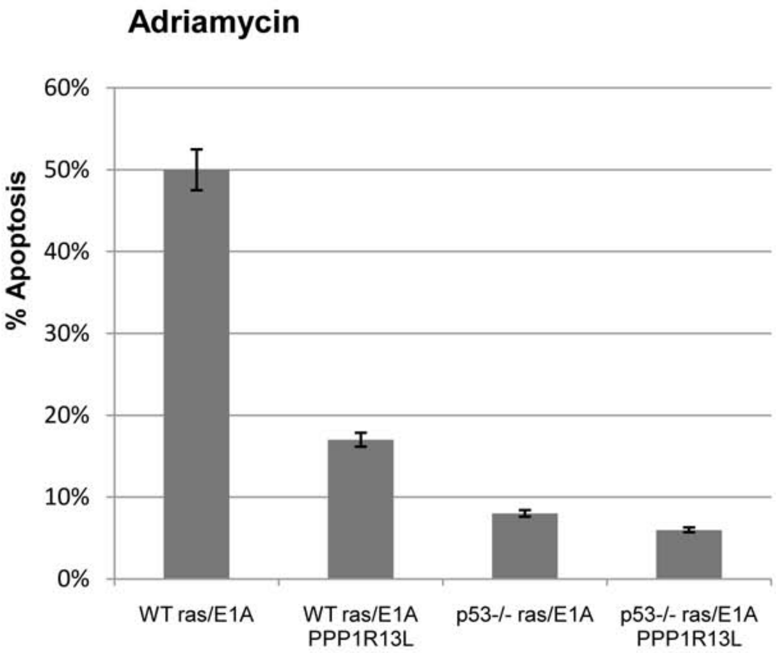
Adriamycin
% Apoptosis
60%
50%
40%
30%
20%
10%
0%
WT ras/E1A
WT ras/E1A PPP1R13L
p53-/- ras/E1A
p53-/- ras/E1A PPP1R13L

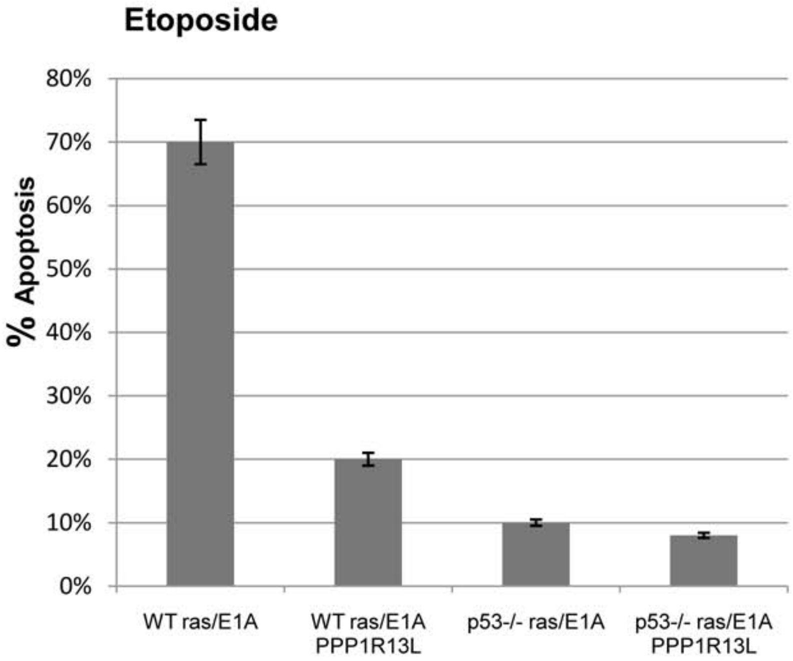
Etoposide
% Apoptosis
80%
70%
60%
50%
40%
30%
20%
10%
0%
WT ras/E1A
WT ras/E1A PPP1R13L
p53-/- ras/E1A
p53-/- ras/E1A PPP1R13L

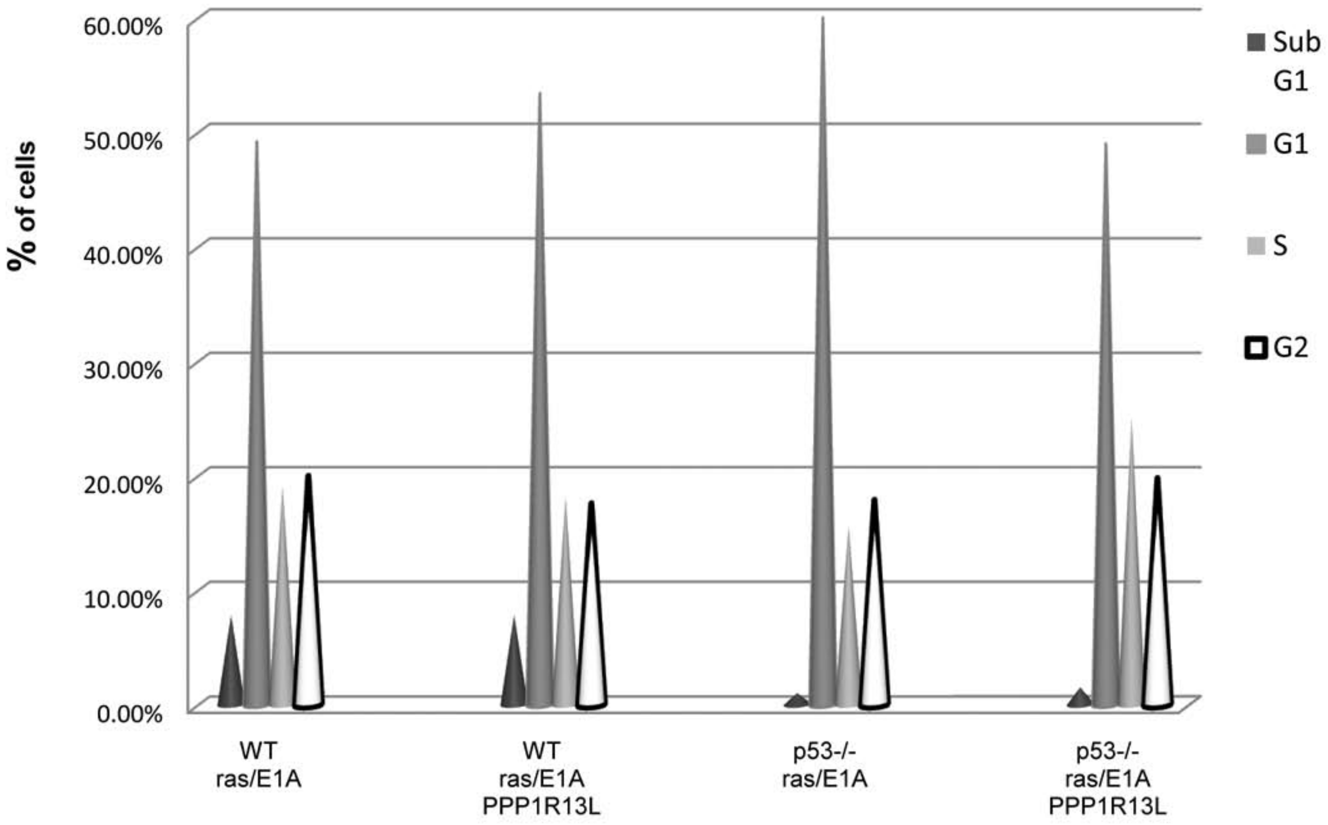
% of cells
60.00%
50.00%
40.00%
30.00%
20.00%
10.00%
0.00%
Sub G1
G1
S
G2
WT ras/E1A
WT ras/E1A PPP1R13L
p53-/- ras/E1A
p53-/- ras/E1A PPP1R13L

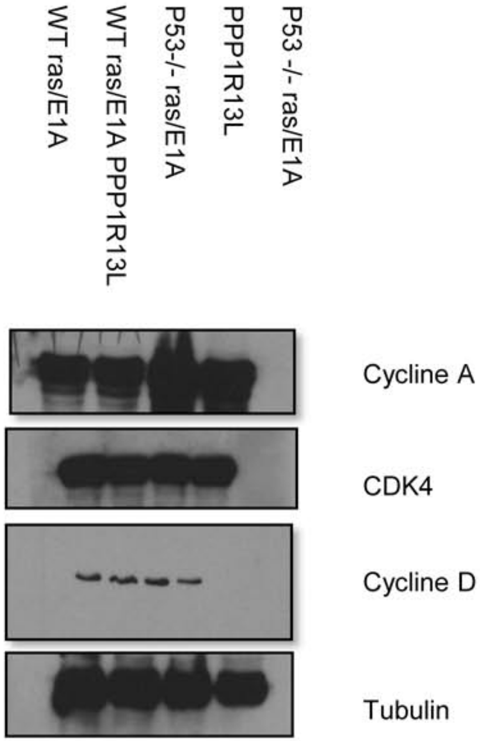
WT ras/E1A
WT ras/E1A PPP1R13L
P53-/- ras/E1A
PPP1R13L
P53 -/- ras/E1A
Cycline A
CDK4
Cycline D
Tubulin

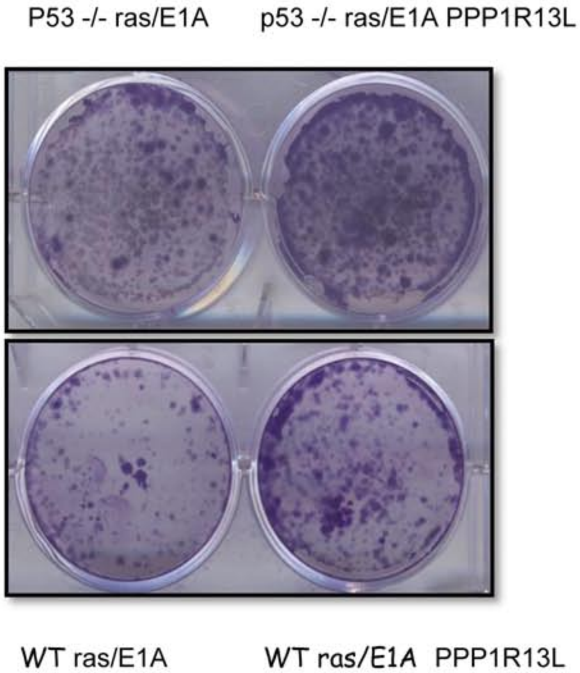
P53 -/- ras/E1A
p53 -/- ras/E1A PPP1R13L
WT ras/E1A
WT ras/E1A PPP1R13L

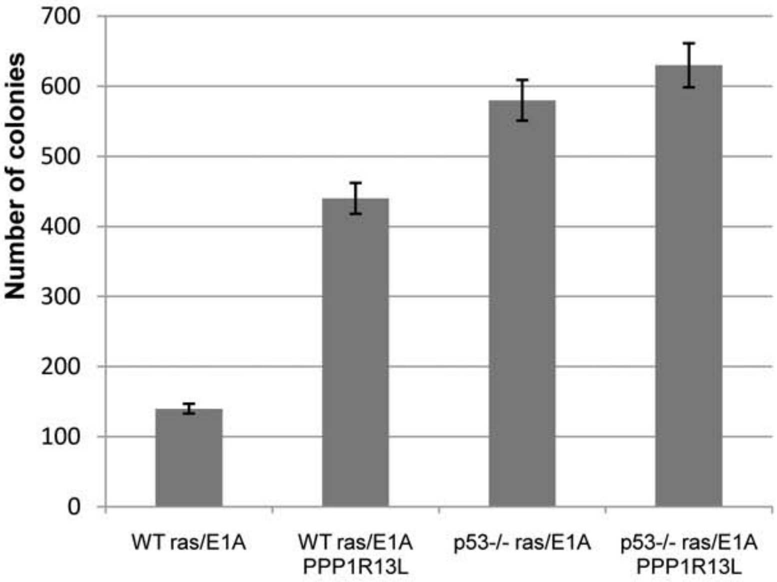
Number of colonies
700
600
500
400
300
200
100
0
WT ras/E1A
WT ras/E1A PPP1R13L
p53-/- ras/E1A
p53-/- ras/E1A PPP1R13L

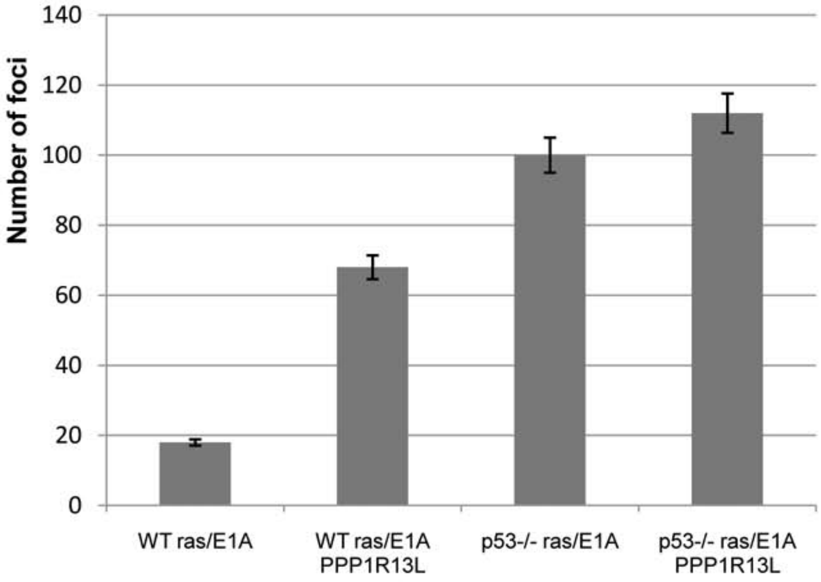
Number of foci
140
120
100
80
60
40
20
0
WT ras/E1A
WT ras/E1A PPP1R13L
p53-/- ras/E1A
p53-/- ras/E1A PPP1R13L

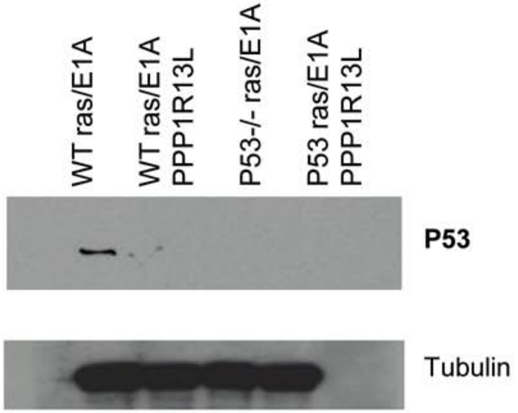
WT ras/E1A
WT ras/E1A PPP1R13L
P53-/- ras/E1A
P53 ras/E1A PPP1R13L
P53
Tubulin

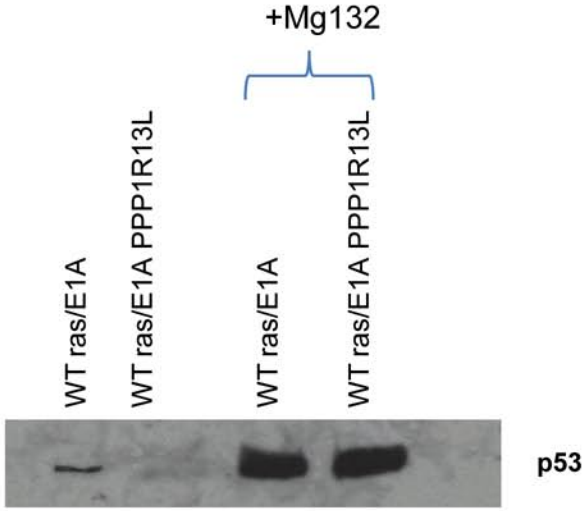
+Mg132
WT ras/E1A
WT ras/E1A PPP1R13L
WT ras/E1A
WT ras/E1A PPP1R13L
p53

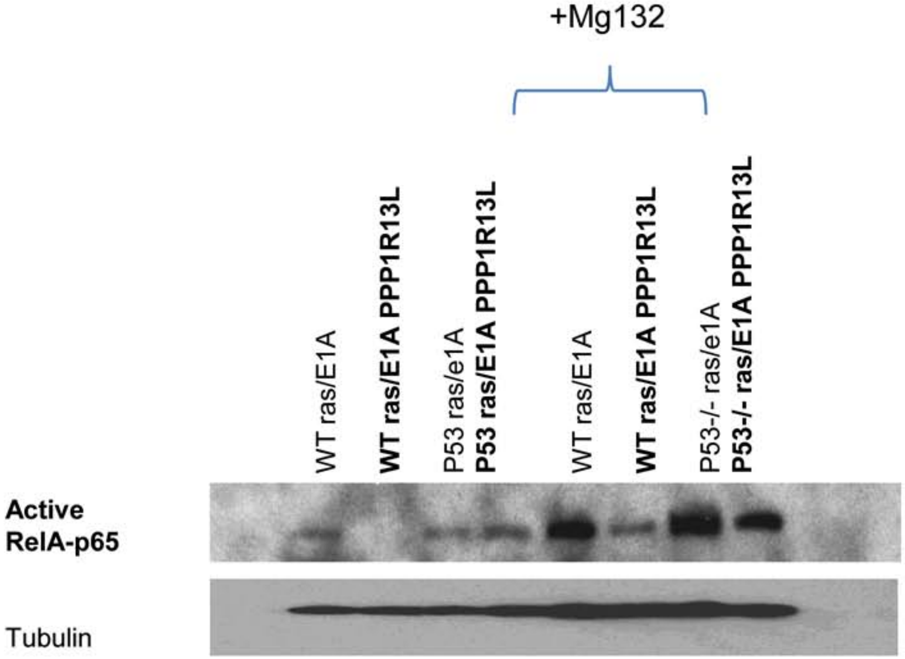
+Mg132
WT ras/E1A
WT ras/E1A PPP1R13L
P53 ras/e1A
P53 ras/E1A PPP1R13L
WT ras/E1A
WT ras/E1A PPP1R13L
P53-/- ras/e1A
P53-/- ras/E1A PPP1R13L
Active RelA-p65
Tubulin

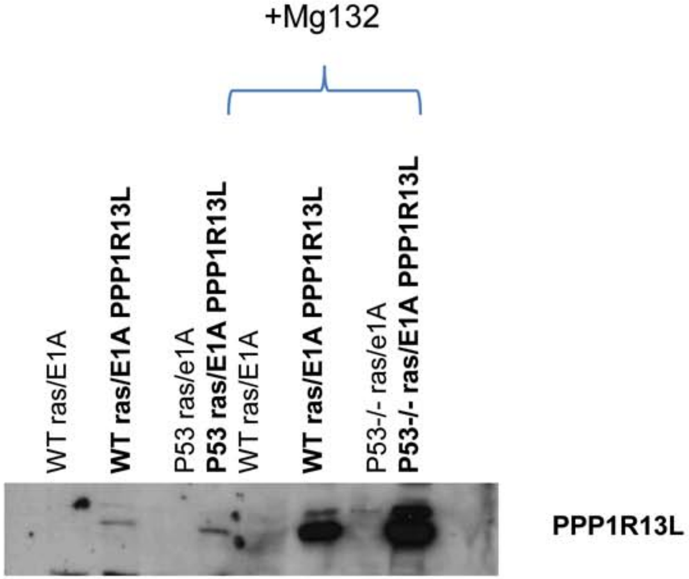
+Mg132
WT ras/E1A
WT ras/E1A PPP1R13L
P53 ras/e1A
P53 ras/E1A PPP1R13L
WT ras/E1A
WT ras/E1A PPP1R13L
P53-/- ras/e1A
P53-/- ras/E1A PPP1R13L
PPP1R13L

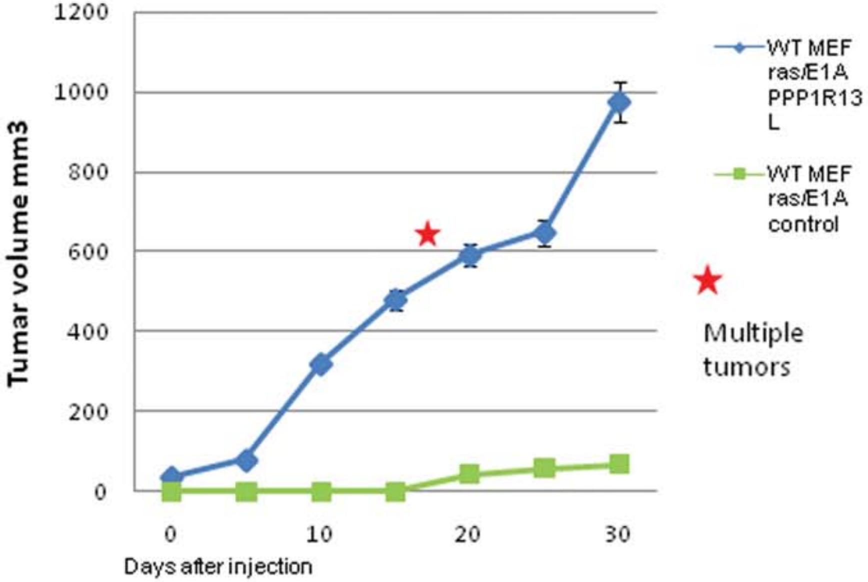

Representative tumor growth curves for WT ras/E1Acontrol and PPP1R13L.

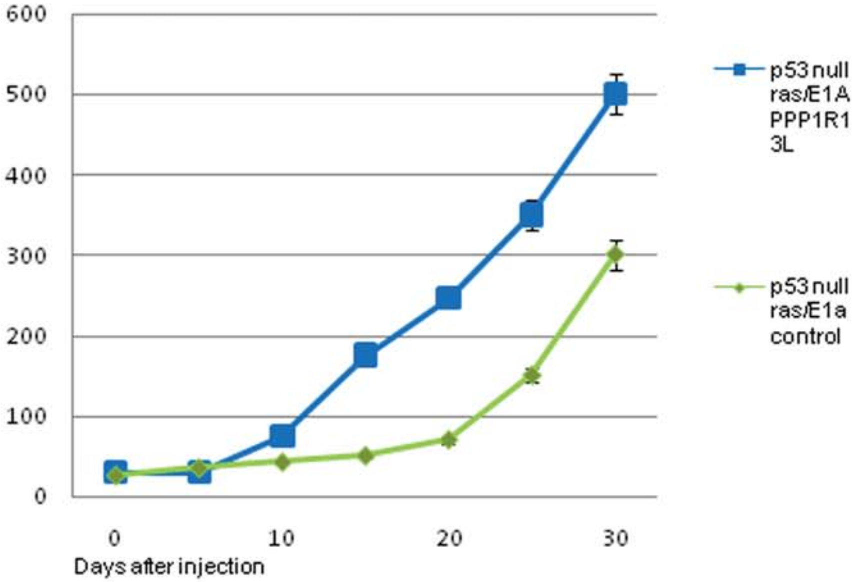

Representative tumor growth curves for p53 null ras/E1Acontrol and PPP1R13L.

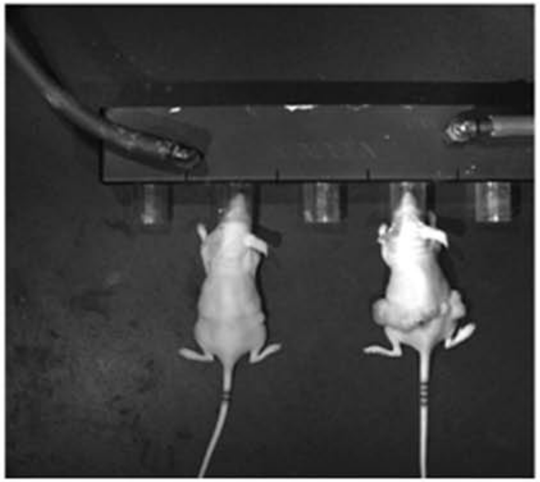

WT ras/E1A control WT ras/E1A PPP1R13L

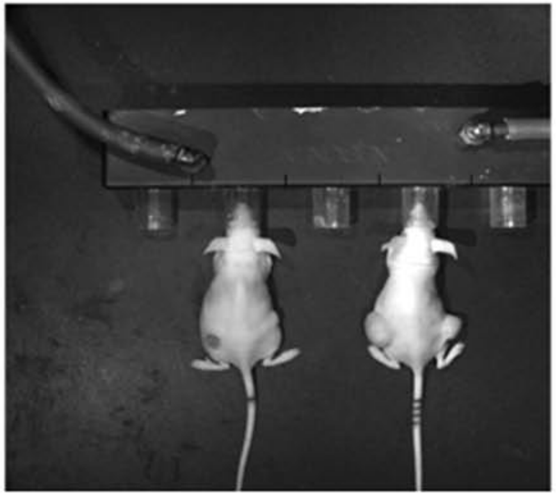

p53-/- ras/E1A control p53-/- ras/E1A PPP1R13L

WT ras/E1A

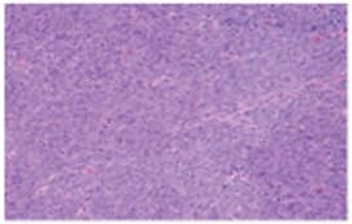

WT ras/E1A PPP1R13L

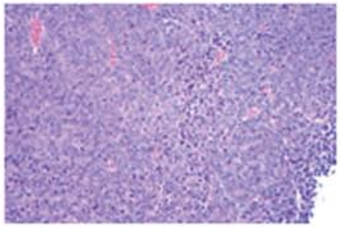

WT ras/E1A

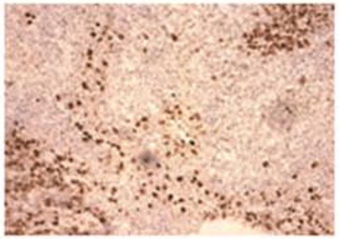

WT ras/E1A PPP1R13L

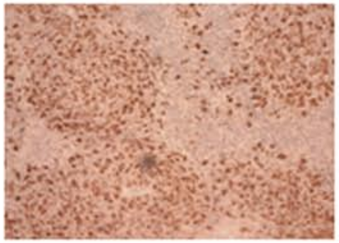

P53 -/- ras/E1A

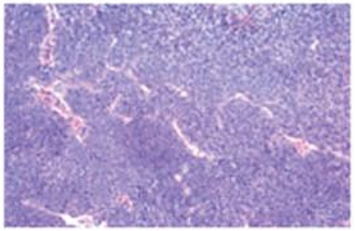

P53-/- ras/E1A PPP1R13L

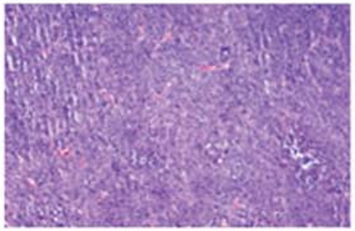

p53-/- ras/E1A

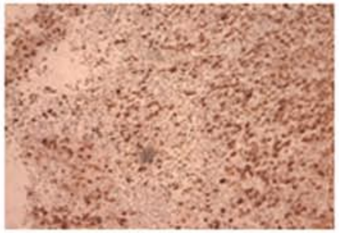

P53-/- ras/E1A PPP1R13L

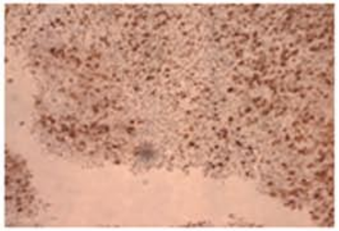

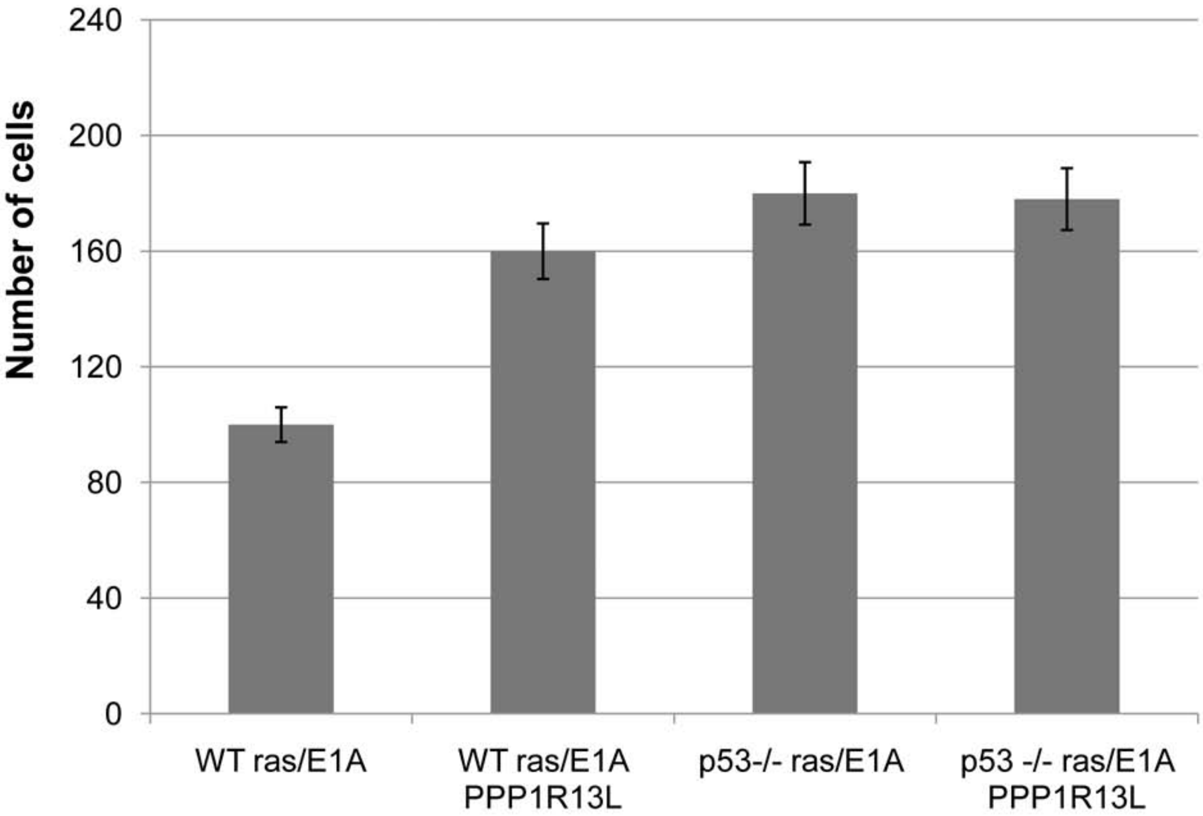
Number of cells
240
200
160
120
80
40
0
WT ras/E1A
WT ras/E1A PPP1R13L
p53-/- ras/E1A
p53 -/- ras/E1A PPP1R13L

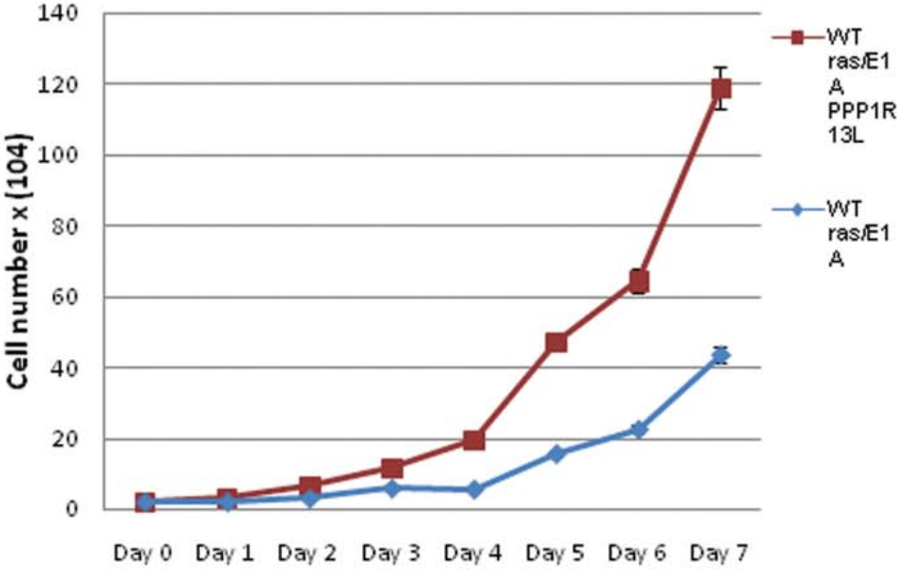
Cell number x (104)
0
20
40
60
80
100
120
140
Day 0
Day 1
Day 2
Day 3
Day 4
Day 5
Day 6
Day 7
WT ras/E1A PPP1R13L
WT ras/E1A

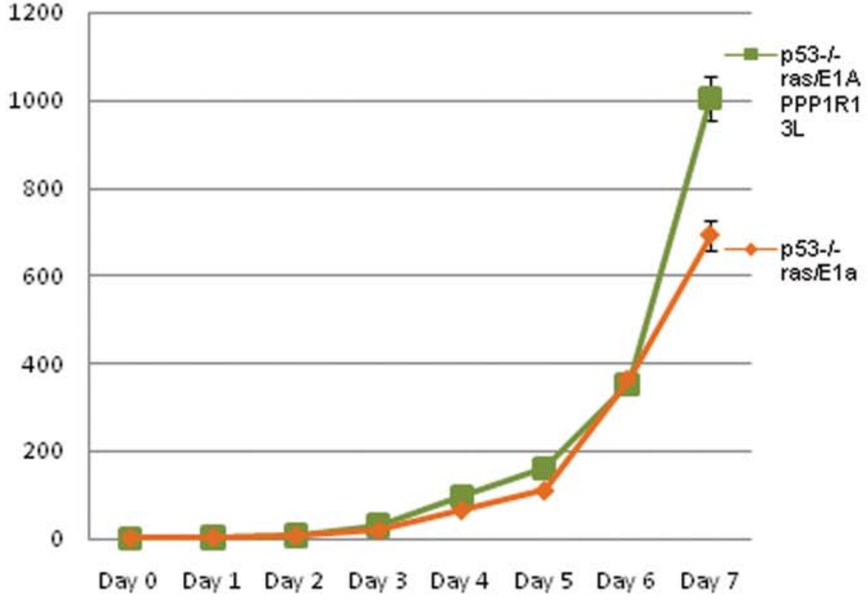
0
200
400
600
800
1000
1200
Day 0
Day 1
Day 2
Day 3
Day 4
Day 5
Day 6
Day 7
p53-/- ras/E1A PPP1R13L
p53-/- ras/E1a

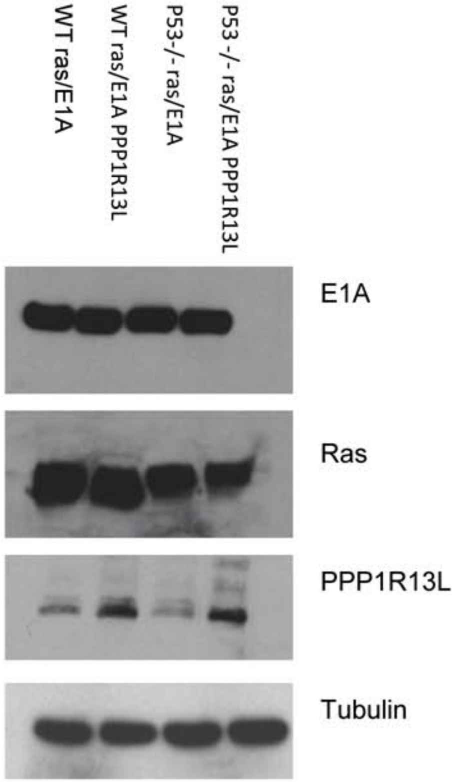
WT ras/E1A
WT ras/E1A PPP1R13L
P53-/- ras/E1A
P53 -/- ras/E1A PPP1R13L
E1A
Ras
PPP1R13L
Tubulin

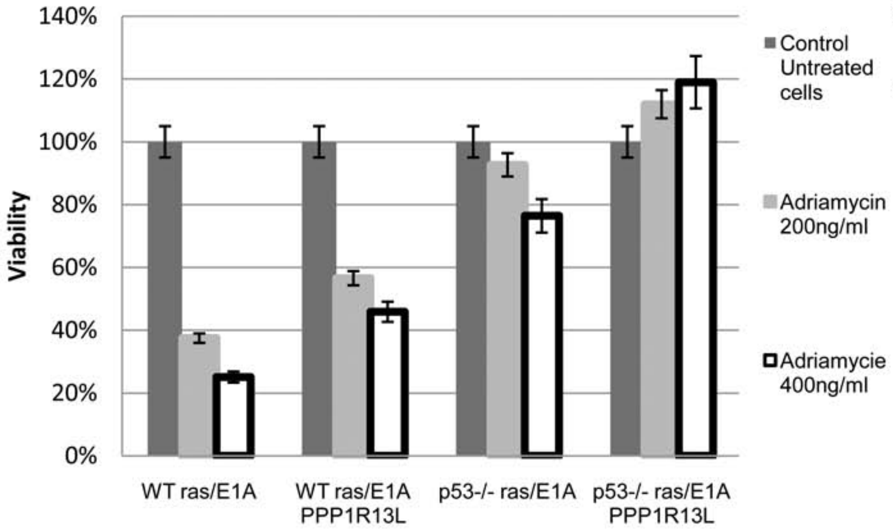
140%
120%
100%
80%
60%
40%
20%
0%
Viability
WT ras/E1A
WT ras/E1A PPP1R13L
p53-/- ras/E1A
p53-/- ras/E1A PPP1R13L
Control Untreated cells
Adriamycin 200ng/ml
Adriamycie 400ng/ml

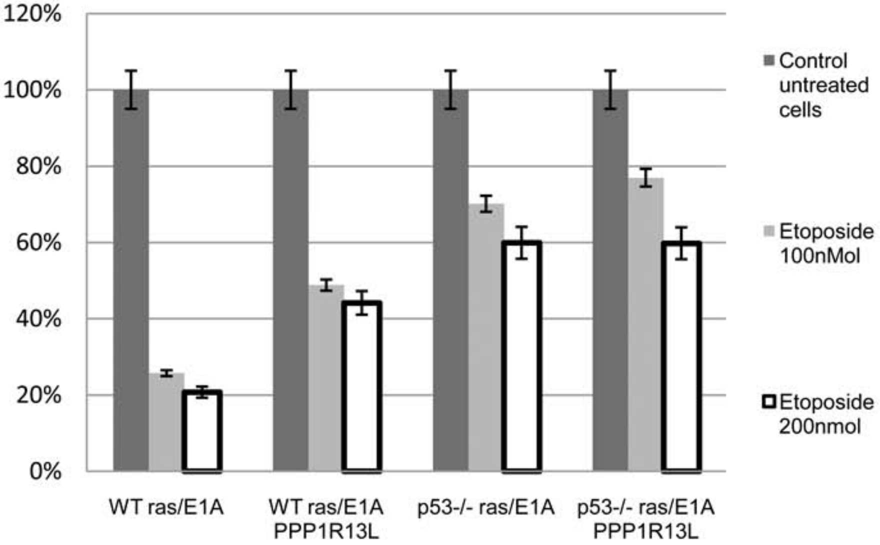
120%
100%
80%
60%
40%
20%
0%
WT ras/E1A
WT ras/E1A PPP1R13L
p53-/- ras/E1A
p53-/- ras/E1A PPP1R13L
Control untreated cells
Etoposide 100nMol
Etoposide 200nmol

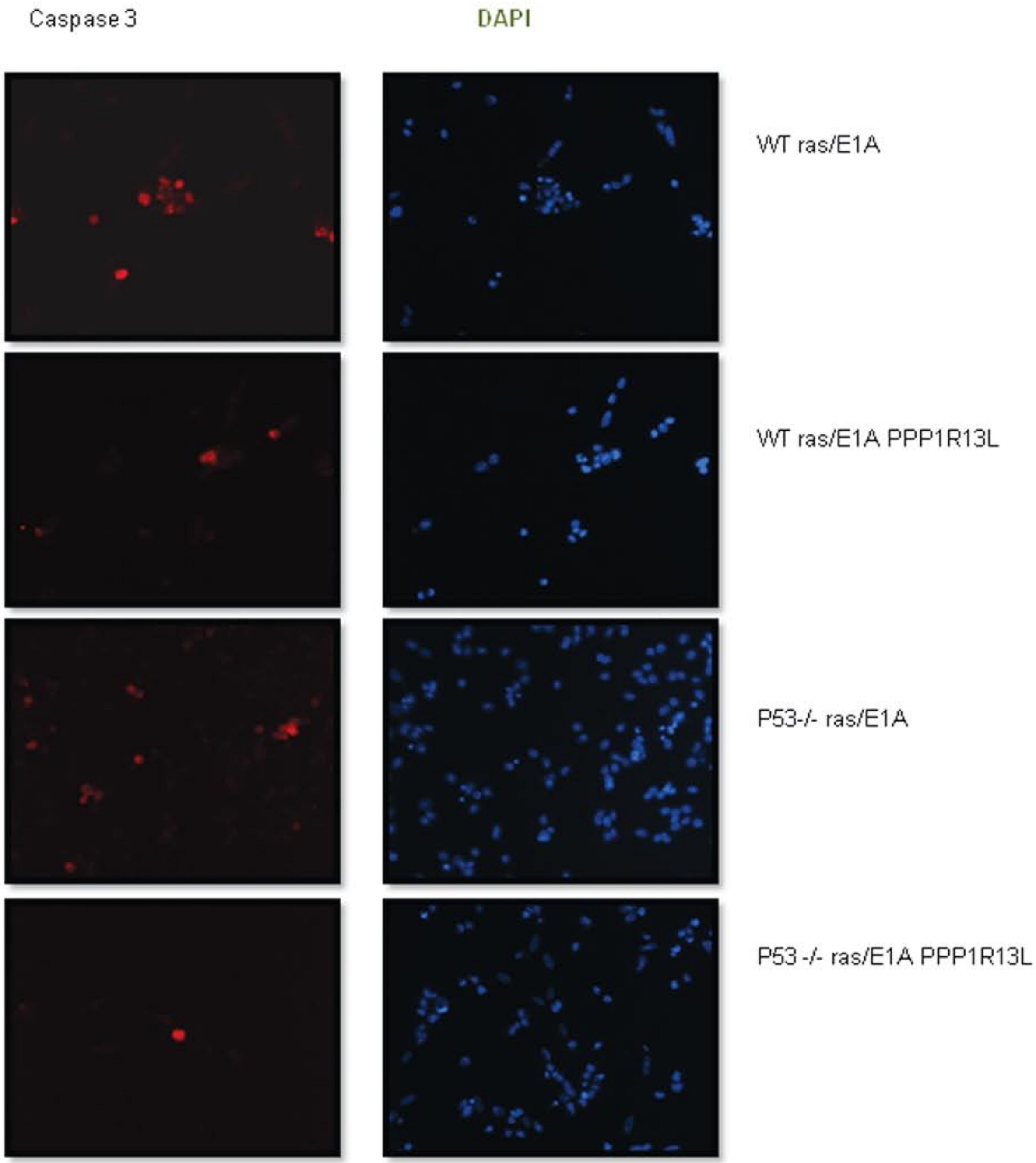
Caspase 3
DAPI
WT ras/E1A
WT ras/E1A PPP1R13L
P53-/- ras/E1A
P53 -/- ras/E1A PPP1R13L

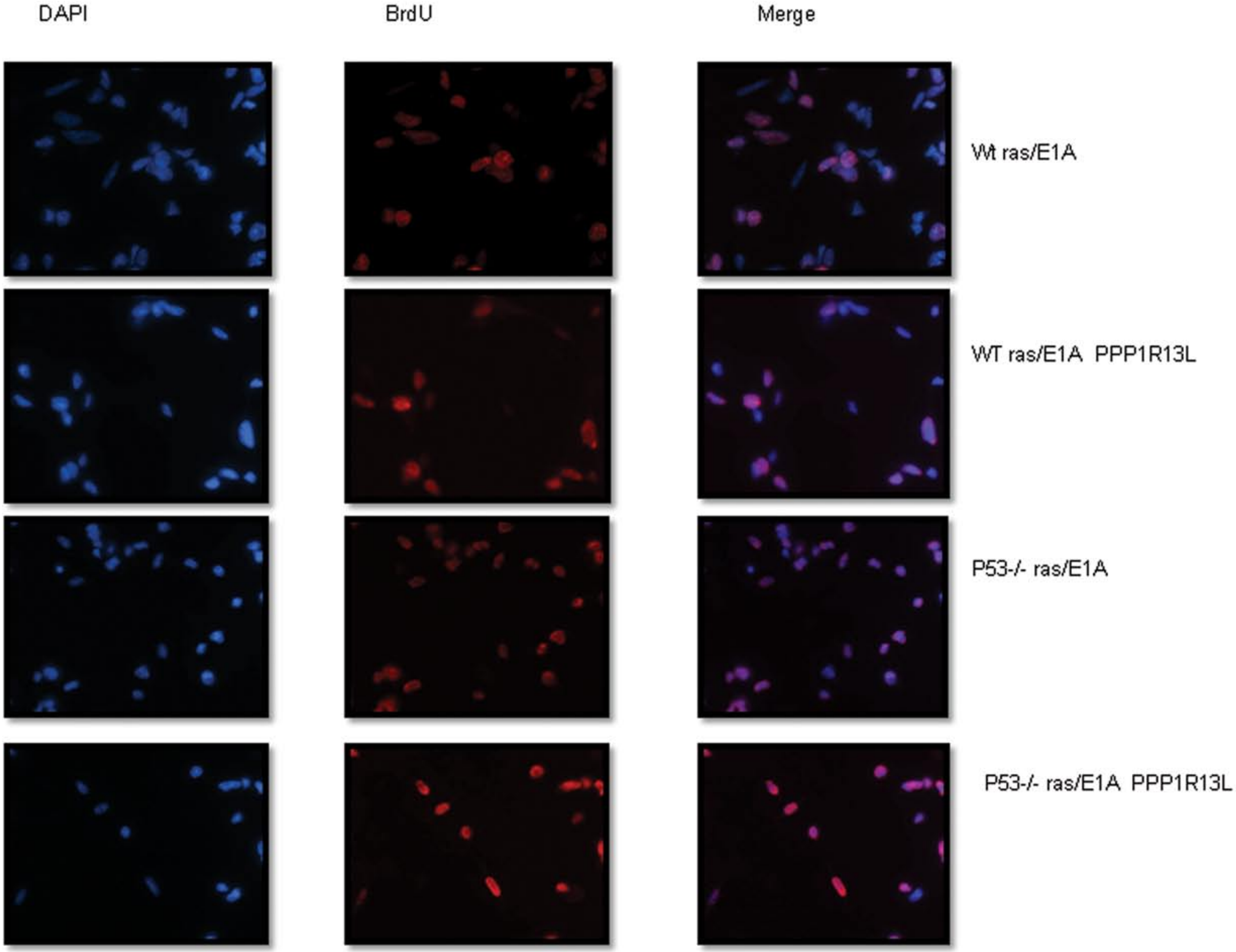
DAPI
BrdU
Merge
Wt ras/E1A
WT ras/E1A PPP1R13L
P53-/- ras/E1A
P53-/- ras/E1A PPP1R13L

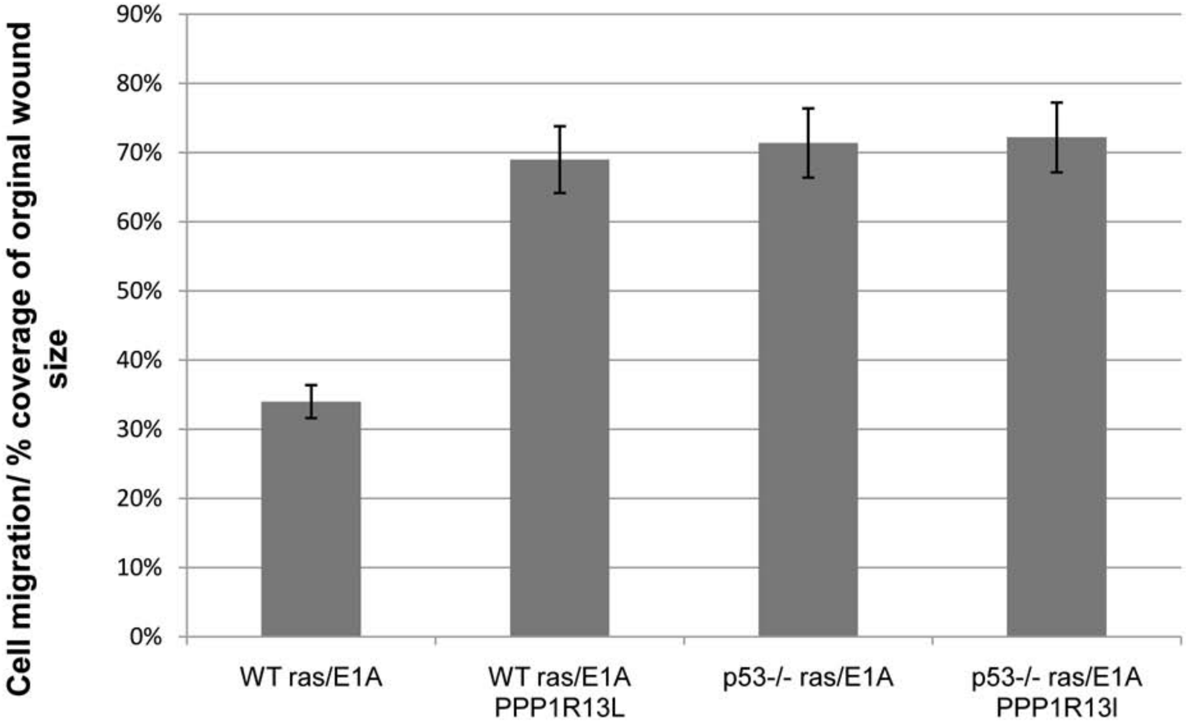
Cell migration/ % coverage of orginal wound size
90%
80%
70%
60%
50%
40%
30%
20%
10%
0%
WT ras/E1A
WT ras/E1A PPP1R13L
p53-/- ras/E1A
p53-/- ras/E1A PPP1R13l

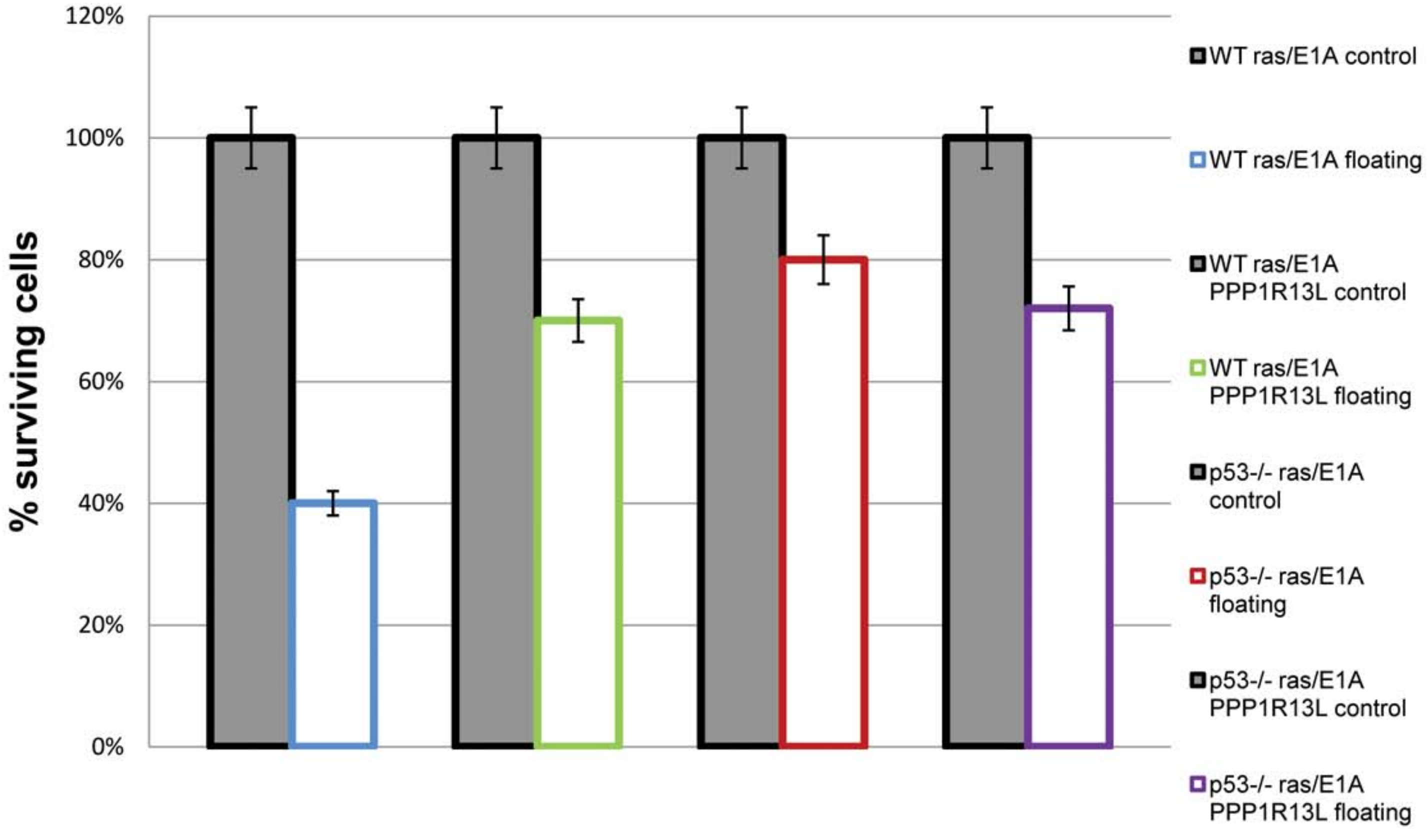
% surviving cells
120%
100%
80%
60%
40%
20%
0%
WT ras/E1A control
WT ras/E1A floating
WT ras/E1A PPP1R13L control
WT ras/E1A PPP1R13L floating
p53-/- ras/E1A control
p53-/- ras/E1A floating
p53-/- ras/E1A PPP1R13L control
p53-/- ras/E1A PPP1R13L floating

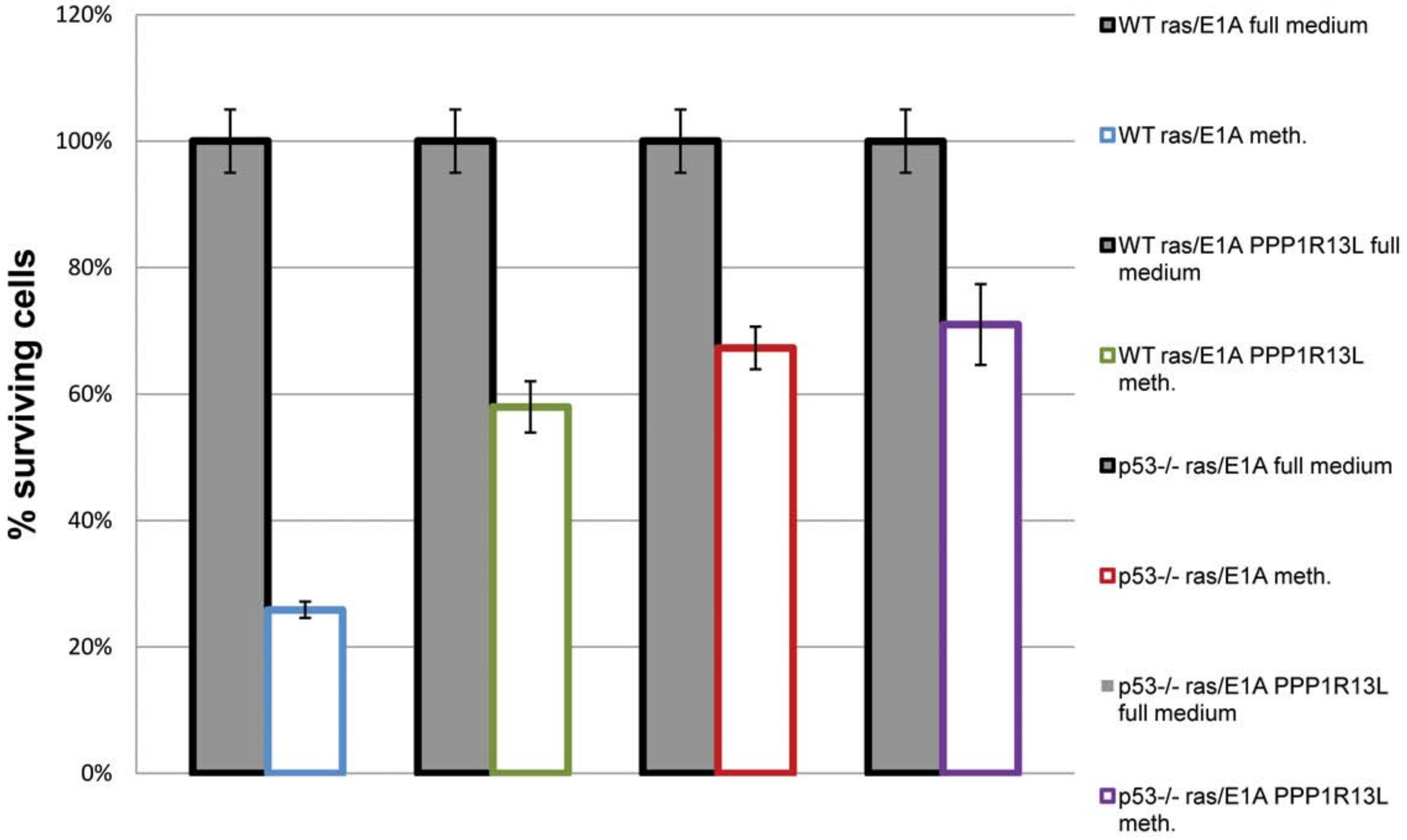
120%
100%
80%
60%
40%
20%
0%
% surviving cells
WT ras/E1A full medium
WT ras/E1A meth.
WT ras/E1A PPP1R13L full medium
WT ras/E1A PPP1R13L meth.
p53-/- ras/E1A full medium
p53-/- ras/E1A meth.
p53-/- ras/E1A PPP1R13L full medium
p53-/- ras/E1A PPP1R13L meth.